DOI: 10.1002/chem.200500999

Pyrene as Chromophore and Electrophore: Encapsulation in a Rigid Polyphenylene Shell

Stefan Bernhardt, Marcel Kastler, Volker Enkelmann, Martin Baumgarten, and Klaus Müllen*[a]

Abstract: Starting from the fourfold ethynyl-substituted chromophore 1,3,6,8-tetraethynylpyrene as core, a series of polyphenylene dendrimers was prepared in high yield by combining divergent and convergent growth methods. The fluorescence quantum yields ($Q_f > 0.92$) of the encapsulated pyrene chromophore were independent of the size of the polyphenylene shell. Fluorescence quenching studies and temperature-dependent fluorescence spectroscopy were performed to investigate the site isolation of the core. They indicate that a second-generation dendrimer layer is needed to efficiently shield the encapsulated pyrene and prevent aggregate formation. Alkali-metal reduction of the encapsulated pyrene core was carried out to afford the corresponding pyrene radical anions, for which hampered electron transfer to the core was observed with increasing dendrimer generation, which is further proof of the site isolation due to the polyphenylene shell. To improve film formation and solubility of the material, solubilizing alkyl chains were introduced on the periphery of the spherical particles. Furthermore, highly transparent films obtained by a simple drop-casting method showed blue emission mainly from the unaggregated species. The materials presented herein combine high quantum efficiency, good solubility, and improved film-forming properties, which make them possible candidates for several applications in electronic devices.

Keywords: dendrimers · EPR spectroscopy · fluorescence · pyrenes · substituent effects

Introduction

The fluorescence properties of pyrene are well known and characterized by long excited-state lifetimes[1] and distinct solvatochromic shifts.[2] Furthermore, pyrene exhibits characteristic excimer formation in concentrated solutions and in the solid state, due to self-association of the polyaromatic hydrocarbon moieties. However, this leads to a dramatic decrease in fluorescence and also to less defined, broadened fluorescence spectra. Therefore, excimer formation of pyrene can be used to study aggregation phenomena.[1b,3] In addition, the sensitive solvatochromic shift of pyrene has been used to exploit the inner structure and polarity of dendrimers by introducing pyrene in the exterior, interior, or throughout the dendritic structure.[4] Moreover, monolayers and thin films containing pyrene derivatives turned out to be promising candidates for several applications such as organic light-emitting diodes (OLEDs).[5]

Polyphenylene dendrimers have attracted great attention due to their highly stiff and shape-persistent dendritic backbones[6] on the nanometer scale. Furthermore, this class of dendrimers can be synthesized strictly monodisperse in high yields, and this allows accurate control over the size of the resulting spherical macromolecules. Recently, we have shown that by attaching polyphenylene dendrons of different generations, an encapsulated perylene chromophore can be shielded from the surrounding medium.[7] However, a significant decrease in fluorescence quantum yield was observed with increasing dendrimer generation. Moore and others combined luminescent chromophores with phenylacetylene dendrons and found energy transfer from peripherally attached donors to the emitting core.[8] Likewise, excitation of polyphenylene dendrons leads to emission of encapsulated perylene, giving rise to an extra excitation band in the UV region.[7a,9]

Insight into the relationship between dendrimer structure and core encapsulation can be derived from investigation of encapsulated redox-active core moieties. For example, a de-

[a] S. Bernhardt, M. Kastler, Dr. V. Enkelmann, Dr. M. Baumgarten, Prof. Dr. K. Müllen
Max-Planck-Institut für Polymerforschung
Ackermannweg 10, 55128 Mainz (Germany)
Fax: (+49) 6131-379-351
E-mail: muellen@mpip-mainz.mpg.de

Supporting information for this article is available on the WWW under http://www.chemeurj.org/ or from the author.

creased reversibility of electrochemical charge transfer has often been correlated with increasing dendrimer generation. Porphyrin is perhaps the most investigated example of a redox-active core to which different types of dendrimer arms have been attached.[10] In this regard, Gorman et al.[11] found that a rigid dendritic architecture hampered the electron-transfer rate to a iron sulfur core much more than a flexible architecture.

Herein the encapsulation of a pyrene moiety in polyphenylene dendrimers of different sizes is described. This is expected to separate the chromophores from each other due to the stiff dendritic arms and therefore suppress aggregation in solution and in the solid state. Since amorphous glassy films are a prerequisite for several electronic devices, a large number of peripherally attached, branched alkyl chains was introduced to improve the film-forming ability of the dendronized pyrenes. The influence of the polyphenylene dendrons on the optical properties of the pyrene core was investigated by UV/Vis absorption and fluorescence spectroscopy. Additional insight into the relationship between dendrimer structure and core encapsulation was derived from alkali-metal reduction of the pyrene dendrimers with pyrene as electrophore.

Results

Synthesis and characterization: To ensure a dense and therefore highly shielding polyphenylene shell around the pyrene core, a large number of starting points for dendrimer growth is desired. Thus, fourfold bromination of pyrene (**1**) in the 1,3,6,8-positions was carried out according to the literature[12] to obtain **2** (Scheme 1).

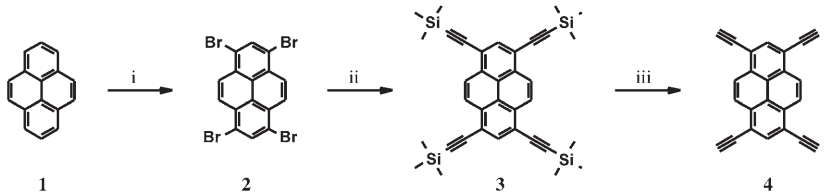

Scheme 1. Synthesis of 1,3,6,8-tetraethynylpyrene (**4**). i) Bromine, nitrobenzene, 160 °C, 90 %; ii) 6 equiv trimethysilylethyne, $[PdCl_2(PPh_3)_2]$, PPh_3, CuI, toluene/triethylamine, 80 °C, 83 %; iii) 8 equiv K_2CO_3, methanol, 95 %.

Hagihara–Sonogashira[13] cross-coupling of **2** with trimethysilylethyne afforded **3** in 83 % yield, which was deprotected with K_2CO_3 in methanol to give activated pyrene core **4** in high yield. The preparation of structurally defined polyphenylene dendrimers with a pyrene core was realized by repetitive coupling and activation steps based on Diels–Alder cycloadditions[14] (Scheme 2). Despite of the low solubility of **4**, first-generation dendrimer **6** was obtained by Diels–Alder cycloaddition with tetraphenylcyclopentadienone (**5**) in quantitative yield.

Since the shielding of the encapsulated pyrene core was expected to increase with increasing dendrimer generation, the unsubstituted second- to fourth-generation dendrimers (**11**, **20**, **21**) were synthesized by repetitive cycloadditions of the branching unit 3,4-bis(4-triisopropylsilyethynylphenyl)-2,5-diphenylcyclopentadienone[15] (**8**) and quantitative desilylation of the protecting groups with tetrabutylammonium fluoride (TBAF; Scheme 3).

Third-generation dendrimer **20** was synthesized by a combination of convergent and divergent synthetic steps: firstly, synthesis of second-generation dendron **19**[16] and, secondly, reaction of **19** with ethynyl-substituted first-generation dendrimer **10**. Due to the higher steric demand of dendron **19**, the yield of the Diels–Alder cycloaddition step was reduced. To improve the film-formation ability and thus reduce the crystallinity of the materials, alkyl chains were introduced into second-generation derivative **11b** by using the corresponding alkyl-substituted tetraphenylcyclopentadienone **14**. These alkyl chains lowered significantly the isotropization temperature of liquid-crystalline polyaromatic hydrocarbons, and much higher solubility was observed.[17] Cyclopentadienone **14** was obtained by oxidation of substituted diphenylacetylene **12** to corresponding benzil derivative **13** and subsequent Knoevenagel condensation with 1,3-diphenylpropan-2-one.

All higher generation dendrimers have good solubility in common organic solvents, (e.g., **15** even in hexane) which allows purification by column chromatography and full characterization by standard spectroscopic techniques. The ^{1}H NMR spectra showed well-separated and clearly assignable signals for the aromatic pyrene protons, as well as for the ethynyl or triisopropylsilyl (TiPS) protons. For the higher generation dendrimers, not all the aromatic signals could be distinguished due to strong signal overlap. In the case of the ethynyl- and TiPS-substituted dendrimers, the intensity ratios between aromatic and aliphatic signals corresponded to the expected values. As an additional proof of structure, the single proton on the pentaphenyl repeating units (see Scheme 2) was used, since generation-dependent chemical shifts were observed. The monodispersity of the described dendrimers could easily be verified by MALDI-TOF mass spectrometry. For all dendrimers, the calculated and experimentally determined m/z ratios were in good agreement, even for fourth-generation dendrimer **21** with a molecular weight of 23031 g mol^{-1}.

The growth of single crystals of suitable size and perfection is often difficult, mainly due to the conformational flexibility of most dendritic backbones.[18] To gain further insight into the spatial arrangement of the shielding polyphenylene dendrons, first-generation dendrimer **23** bearing an additional phenyl group on each dendritic branch was synthesized

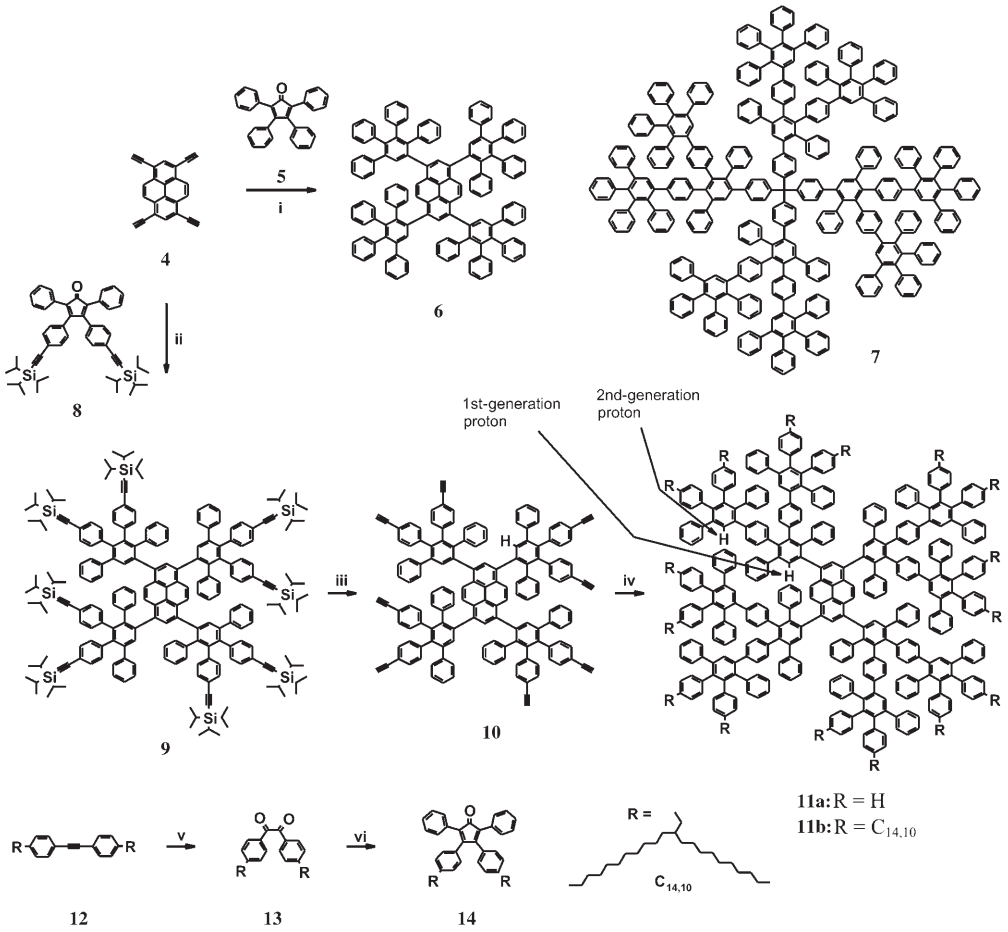

Scheme 2. Synthesis of first- and second-generation dendrimers **6**, **11a**, and **11b**. Polyphenylene dendrimer **7** constructed from tetrahedral tetraphenylmethane as core.[15] i) 6 equiv **5**, *o*-xylene, 160 °C, 95 %; ii) 6 equiv **8**, *o*-xylene, 160 °C, 71 %; iii) TBAF, THF, 93 %; iv) **11a**: 16 equiv **5**, *o*-xylene, 160 °C, 73 %; **11b**: 14 equiv **14**, Ph_2O, 220 °C, 63 %. v) 1 equiv I_2, DMSO, 170 °C, 40 %; vi) 1 equiv 1,3-diphenylpropan-2-one, *tert*-butanol, 80 °C, 49 %.

(Scheme 4). Due to the higher molecular symmetry of **23**, a more pronounced tendency towards crystallization was expected. Hagihara–Sonogashira cross-coupling of **2** with phenylacetylene gave 1,3,6,8-tetrakis(phenylethynyl)pyrene (**22**). Subsequent Diels–Alder reaction with tetraphenylcyclopentadienone (**5**) yielded first-generation dendrimer **23**.

Crystals of **23** suitable for structure determination were obtained from CH_2Cl_2 solution by slow evaporation at room temperature.[19] A projection of the crystal structure is shown in Figure 1.

The crystal contains eight well-ordered CH_2Cl_2 molecules per dendrimer unit. The four central phenyl rings of the pentaphenylbenzene substituents are oriented approximately perpendicular to the pyrene core. Thus, the dendrimer assumes the shape of a cross.

UV/Vis and EPR spectroscopic studies: In the absorption spectra of the first- to fourth-generation dendrimers **6**, **11a**, **20**, and **21** two distinct bands, one in the visible region (ca. 395 nm) and the other in the UV region (280–350 nm), were observed (Figure 2).[20]

The absorption in the visible region is due to the π–π* transition of the pyrene core and showed a red-shift of up to 55 nm compared with unsubstituted pyrene (337 nm), in accord with other phenyl-substituted pyrenes, for example, 1,3,6,8-tetraphenylpyrene (380 nm).[21] Additionally, the fine structure of the pyrene absorption spectrum was lost due to substitution with phenyl rings. The absorption band in the UV region can be predominantly attributed to the polyphenylene dendrons,[7a,9] as indicated by the linear increase in the extinction coefficients $\varepsilon(\lambda)$ with increasing number of attached phenylene moieties. Going to higher generations has no influence on the absorption maximum and extinction coefficients of the pyrene core.[22]

The emission spectra of **6**, **11a**, **20** and **21** (Figure 2), obtained on excitation of the pyrene core at 390 nm displayed a broad emission band at 425 nm, red-shifted compared to the emission of parent pyrene (395 nm). No change in emission maximum or fluorescence intensity of the pyrene core with changing dendrimer generation was observed. Excitation of the polyphenylene dendrons at 310 nm resulted in strong emission of the pyrene core at 425 nm, which indicates efficient energy transfer from the polyphenylene den-

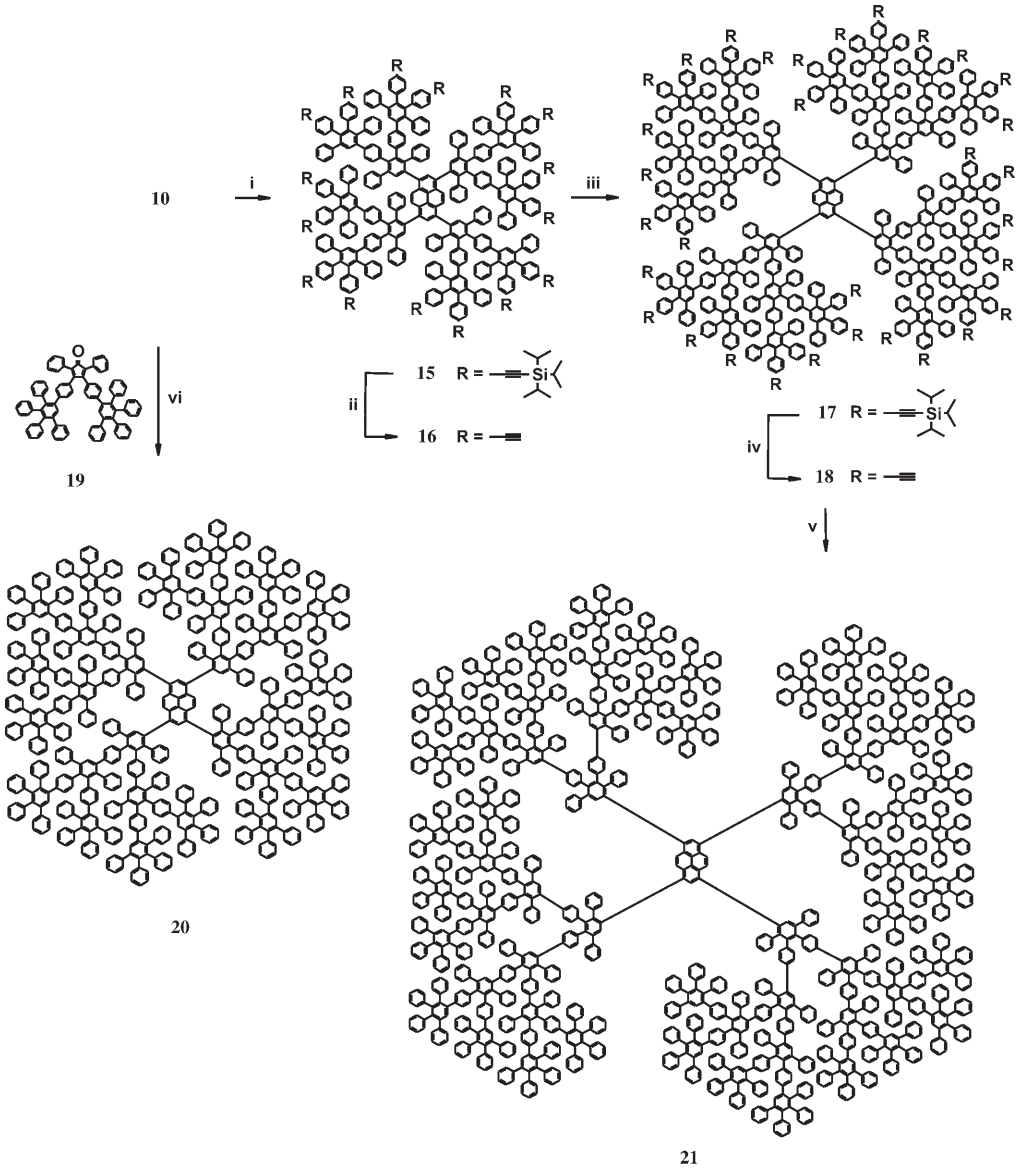

Scheme 3. Synthesis of third- and fourth-generation dendrimers **20** and **21**. i) 12 equiv **8**, *o*-xylene, 150 °C, 76 %; ii) TBAF, THF, 91 %; iii) 32 equiv **8**, *o*-xylene, 160 °C, 85 %; iv) TBAF, THF, 89 %; v) 65 equiv **5**, Ph_2O, 190 °C, 85 %; vi) 16 equiv **19**, *o*-xylene, 170 °C, 55 %.

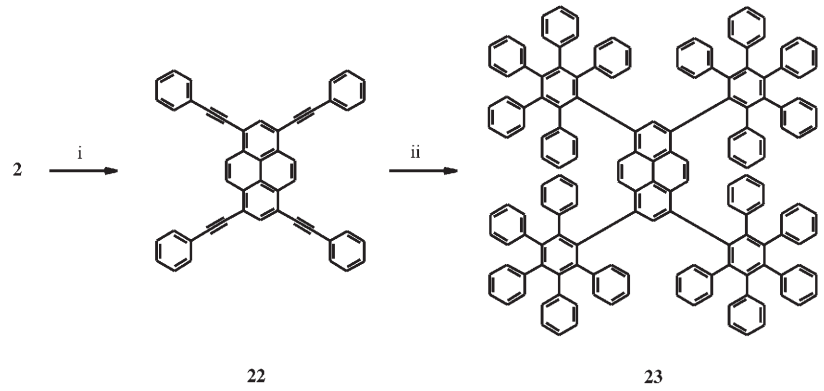

Scheme 4. Synthetic route to first-generation dendrimer **23**. i) 6 equiv phenylacetylene, $[PdCl_2(PPh_3)_2]$, PPh_3, CuI, toluene/triethylamine, 80 °C, 92 %; ii) 6 equiv **5**, Ph_2O, 230 °C, 90 %.

drons to the pyrene core (for further details, see Supporting Information). The fluorescence quantum yields Q_f of **6**, **11a**, **20**, and **21** in $CHCl_3$ were determined by using 9,10-diphenylanthracene as reference chromophore (Table 1).[23]

Pyrene exhibits sensitive solvatochromic behavior in which the relative intensity of emission bands is dependent on solvent polarity.[2a,24] Webber and co-workers used this effect to investigate the diffusion of

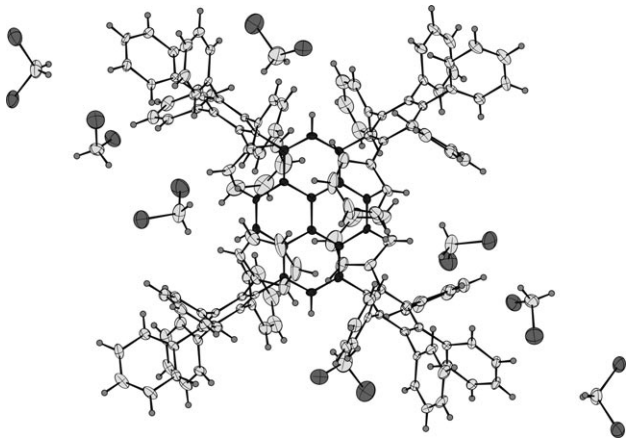

Figure 1. X-ray structure of **23** recrystallized from CH_2Cl_2.

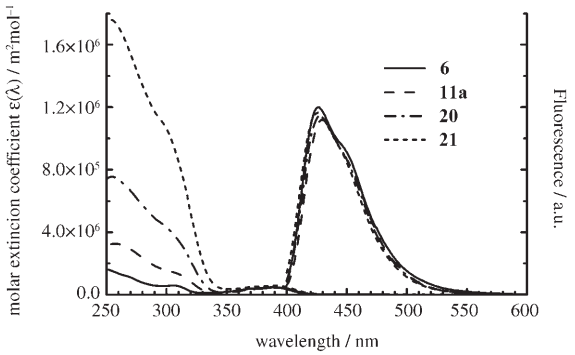

Figure 2. Absorption and emission spectra of dendronized pyrenes **6**, **11a**, **20**, and **21** in $CHCl_3$. Excitation: 390 nm. The emission spectra were normalized to the same optical density at the excitation wavelength.

Table 1. Fluorescence quantum yields of dendronized pyrenes **6**, **11a**, **20**, and **21** in $CHCl_3$.

	6	**11a**	**20**	**21**
Q_f[a]	0.96±0.03	0.97±0.02	0.97±0.03	0.92±0.02

[a] Excitation: 350 nm; errors were estimated by using Gauss's law of propagation of error.

pyrene from block-copolymer micelles.[25] Hecht et al. determined the influence of chain length and solvent polarity on the encapsulation of a poly(ε-caprolactone)-dendronized pyrene.[4b] They found a solvation-induced encapsulation effect, mainly due to the structural extent and collapse of the dendrimer backbone. This should also be tested for polyphenylene-dendronized pyrenes. Accordingly, TiPS-substituted dendrimers **9** and **17** as well as 1,3,6,8-tetraphenylpyrene (TPP) as reference were dissolved in cyclohexane and methanol. The TiPS groups were necessary to ensure solubility of the dendrimers in both solvents. Emission spectra showed a bathochromic shift of the pyrene emission with increasing solvent polarity of $\Delta\lambda = 9$ nm (**9**), 6 nm (**17**), and 9 nm (TPP).

In concentrated solutions ($c > 10^{-4}$ M), pyrene exhibits strong characteristic excimer fluorescence at 475 nm.[26] When solutions of **10** in $CHCl_3$ with different concentrations were excited at 390 nm, a strong decrease in the overall fluorescence intensity was observed with increasing concentration (Figure 3a).

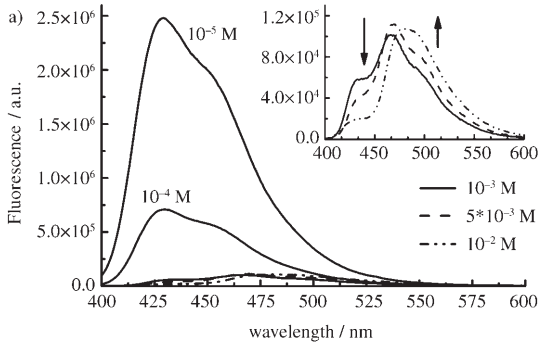

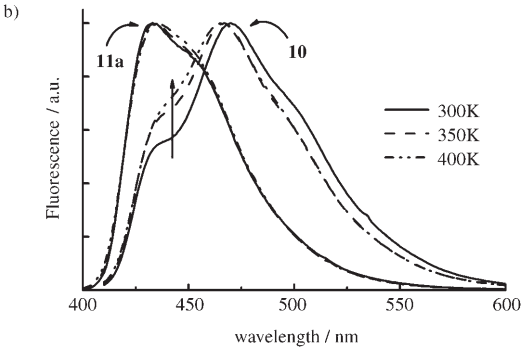

Figure 3. a) Emission spectra of **10** with increasing concentration in $CHCl_3$. Excitation: 390 nm. b) Temperature-dependent fluorescence spectra of dendronized pyrenes **10** and **11a** ($c = 10^{-2}$ M) in tetrachloroethane, normalized to their emission maximum. Excitation: 390 nm.

More detailed inspection of the spectra (inset in Figure 3a) showed a decrease in the emission band at 425 nm and simultaneous increase in emission intensity at 470 nm. This most probably indicates aggregation of the pyrene cores in first-generation dendrimer.

Since the temperature dependence of the monomer–excimer equilibrium can provide information on the steric or electronic environment of the pyrene moiety,[3,27] the temperature-dependent fluorescence spectra of polyphenylene-dendronized pyrenes **10** and **11a** were recorded (excitation at 390 nm, Figure 3b).[28] At room temperature (300 K), a 10^{-2} M solution of **10** in tetrachloroethane displayed a broad emission spectrum with a maximum at 470 nm, which indicates aggregation. A shoulder at 440 nm may be due to emission from the unaggregated species. At 400 K a small increase in the intensity of this band was noted, while strong fluorescence at 470 nm was still detectable. In contrast, second-generation dendrimer **11a** with the same concentration at 300 K showed an emission spectrum ($\lambda_{max} = 436$ nm) almost similar to that of the unaggregated species in dilute solution (compare Figure 2). When the temperature was in-

creased to 400 K no change in spectral shape was observed, and this rules out underlying aggregate fluorescence at lower temperature.

The fluorescence intensity of a fluorophore depends on the natural lifetime of its first excited singlet state and on the rate at which nonradiative processes deactivate it. Quenching processes depend significantly on the location and accessibility of the fluorophore within a macromolecular structure. Therefore, fluorescent probes such as dansyl chloride are used especially in biochemistry to study the various binding sites in large macromolecules.[29] Furthermore, for pyrenyl moieties on the focal point of poly(amido) dendrimers, decreasing Stern–Volmer quenching constants K_{SV} were found with increasing dendrimer generation.[4a] This was attributed to a greater steric congestion with increasing dendron size making the chromophore less accessible. The Stern–Volmer expression: [Eq. (1)]

$$F_0/F = 1+K_{SV}[Q] = 1+\langle k_q\rangle\langle\tau\rangle_0[Q] \quad (1)$$

allows the quenching process to be investigated by measuring the fluorescence intensity in the absence and presence of the quencher, F_0 and F, respectively. In Equation (1), K_{SV} is the Stern–Volmer quenching constant, $\langle k_q\rangle <$ the average bimolecular quenching constant, $\langle\tau\rangle_0$ the mean fluorophore lifetime in the absence of the quencher, and [Q] the analytical concentration of the quencher. Comparing different fluorophores with each other by means of their $\langle k_q\rangle <$ values requires determination of the mean fluorescence lifetime $\langle\tau\rangle_0$.

We used nitromethane and *N*,*N*-dimethylaniline, both well-known quenchers of pyrene fluorescence.[1b] The fluorescence quenching of polyphenylene-dendronized pyrenes and TPP was well described by the Stern–Volmer expression (nitromethane: $r^2>0.996$; *N*,*N*-dimethylaniline: $r^2>0.97$) (Figure 4a,b). By applying Equation (1), the Stern–Volmer quenching constants K_{SV} were determined from the slope of the derived curves.

For nitromethane, the Stern–Volmer quenching constant K_{SV} decreased clearly on going from TPP to first-generation dendrimer **6** and second-generation dendrimer **11a** (Table 2). In particular, no further decrease in K_{SV} was observed for third- and fourth-generation dendrimers **20** and **21**, respectively.

N,*N*-Dimethylaniline as quencher had only a minor influence on the fluorescence intensity of the dendronized pyrenes. Therefore, experimental errors significantly contribute to the obtained curves, as can be seen by the value of $r^2>0.97$. The K_{SV} values, derived from a linear fit, were about 15 times smaller than for nitromethane and decreased significantly only between the first- and the second-generation dendrimers **6** and **11a**, respectively. When tetrachloromethane was used as fluorescence quencher, diverse results were obtained (Figure 4c). Similarly to nitromethane, K_{SV} decreased from TPP to first-generation dendrimer **6**, but a further significant decrease was only observed between third- and fourth-generation dendrimers **20** and **21**, respectively (Table 2).

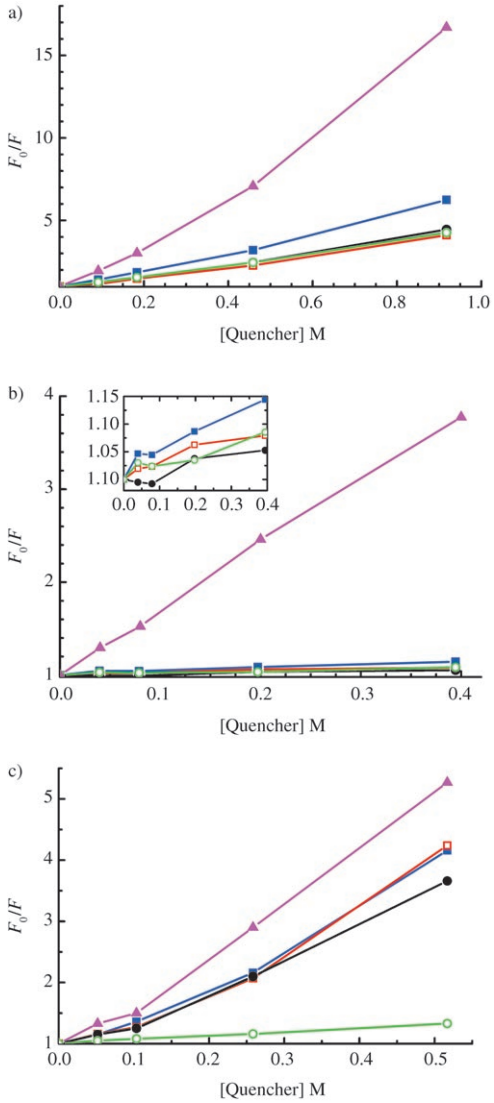

Figure 4. Stern–Volmer quenching plots for a) nitromethane, b) *N*,*N*-dimethylaniline, and c) tetrachloromethane in $CHCl_3$. Excitation: 360 nm. Inset in b): Enlarged plot for *N*,*N*-dimethylaniline. F_0 and F are the fluorescence intensity in the absence and the presence of the quencher, respectively: ■: **6**, □: **11a**, ●: **20**, ○: **21**, ▲: TPP.

Table 2. Stern–Volmer quenching constants K_{SV} for TPP, **6**, **11a**, **20**, and **21** in $CHCl_3$, respectively, obtained with different quenching agents. Excitation: 360 nm.

	K_{SV} [M^{-1}][a]				
	TPP	**6**	**11a**	**20**	**21**
CH_3NO_2	17.27±1.18	5.72±0.28	3.43±0.19	3.77±0.22	3.57±0.12
$C_6H_5N(CH_3)_2$	6.98±0.17	0.33±0.04	0.19±0.03	0.16±0.04	0.19±0.04
CCl_4	8.41±0.42	6.20±0.60	6.35±0.71	5.30±0.35	0.62±0.18

[a] Errors were estimated by using Gauss's law of propagation of error.

The encapsulation effect of the dendronized pyrenes was also tested by means of the electron-transfer behavior of increasingly shielded pyrene cores. Reduction of dendronized pyrenes **11a** and **21** was carried out on a potassium mirror under high vacuum in absolute THF by using a technique previously described.[30] Formation of the charged species was followed by EPR and UV/Vis spectroscopy (for UV/Vis spectra, see Supporting Information). On contact with the potassium mirror the color of the solution of second-generation dendrimer **11a** turned from light yellow to green, and two absorption bands at 456 and 640 nm appeared in the UV/Vis spectrum. This can be ascribed to formation of the radical anion of the substituted pyrene.[31] The disappearance of the absorption band of the neutral starting material at 394 nm on prolonged contact suggested quantitative conversion. The EPR spectroscopic monitoring showed first a broad signal with four shoulders, which should be attributed to the four protons at positions 4, 5, 9, and 10 of the pyrene core ($a_H \approx 0.2$ mT, Figure 5a), whose splittings are very close

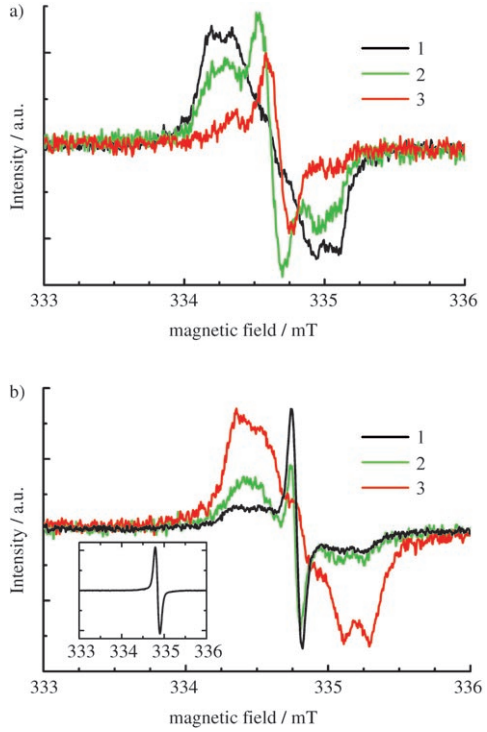

Figure 5. EPR spectra (RT, K, THF) a) **11a** in the order of further reduction 1–3; b) **21** with initial spectrum 1, partial comproportionation 2, and complete comproportionation 3. Inset in b): EPR spectrum for the reduction of **7**.

to those of the corresponding protons of the known pyrene radical anion ($a_H = 0.208$ mT).[32]

On further reduction, the intensity of this signal was diminished, but instead of reaching a diamagnetic dianionic state, a new sharp signal appeared in the center of the spectrum and increased in intensity ($\Delta H_{pp} \approx 0.1$ mT). In a control experiment, second-generation dendrimer **7** was considered for charging. The EPR and UV/Vis spectra of the reduction of **7** were similar to those observed after prolonged reduction of **11a**, namely, a sharp signal (inset in Figure 5b) and absorption maxima at 450 and 750 nm. On reduction of fourth-generation dendrimer **21** a strong sharp signal immediately appeared in the EPR spectrum ($\Delta H_{pp} \approx 0.1$ mT, Figure 5b), as also found for **7**.[33] However, after equilibrating with neutral compound (comproportionation) a broad signal with four shoulders ($a_H \approx 0.2$ mT) was found, similar to the EPR spectrum of **11a**, which strongly supports the assignment of this signal to the radical monoanion of dendronized pyrenes **11a** and **21**. The pyrene radical monoanion could not be observed in the absorption spectra of **21** recorded during reduction, mainly due to unresolved spectra. On further reduction of **21** the sharp line in the EPR spectrum reappeared and revealed close similarity to the control sample **7**. In all three samples the sharp line broadened on prolonged contact with the potassium mirror, but no defined number of transferred electrons could be ascribed ($\Delta H_{pp} \approx 0.6$ mT).

To investigate the solid-state photophysics of dendronized pyrenes, the absorption and fluorescence spectra of alkyl-chain-decorated second-generation dendrimer **11b** were recorded. Films of good optical quality were obtained by simple drop casting and spin coating from toluene solution onto quartz substrates. The transparency of the films of dendrimer **11b** was much higher than for those made from parent pyrene, mainly due to crystallization of the non-dendronized species. Absorption and emission spectra of the films showed a typical broadening relative to solution spectra (Figure 6).

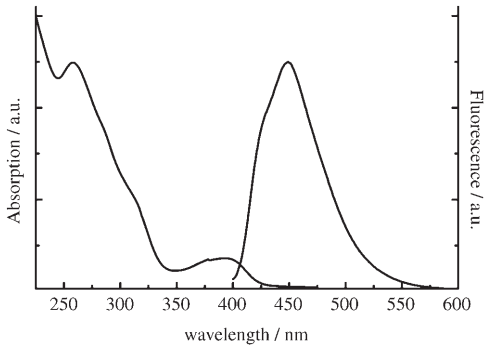

Figure 6. Absorption and emission spectra of **11b** in a film prepared from toluene solution. Excitation: 390 nm.

Thin-film dendrimer **11b** displayed an absorption maximum of at 393 nm, almost unshifted compared with solution spectra. The absorption band in the UV region at 260 nm can be assigned to the polyphenylene dendrons.[7a] Compared with solution (337 nm), the absorption maximum of unsubstituted pyrene in the film (337 nm) was not shifted at all. The emission maximum of the film prepared from unsubstituted pyrene (446 nm) was red-shifted by 51 nm compared to that in solution (395 nm), that is, emission in the

solid state originated mainly from aggregated species (excitation: 390 nm). On the contrary, emission of **11b** occurred at 449 nm, that is, a bathochromic shift of only 20 nm compared with solution spectra.

Discussion

Monodisperse polyphenylene dendrimers with an encapsulated pyrene moiety have been synthesized in high yield starting from tetraethynyl-substituted pyrene core **4**. The crystal structure of the first-generation dendrimer **23** showed that the first-generation polyphenylene shell already produces pronounced steric shielding of the pyrene core. The shape persistence of the polyphenylene dendrons[6] suggests that shielding would be even more pronounced for higher generations. This expectation is indeed born out by the fact that, compared to TPP as reference, third-generation dendrimer **17** showed a less solvatochromically shifted emission maximum. One can attribute this to the creation of a stable hydrophobic environment around the pyrene core, due to the large number of surrounding phenyl rings. In contrast to dendrimers constructed from flexible building units, the shape and conformation of the stiff polyphenylene dendrons do not change with changing polarity of the surrounding medium.

No decrease in fluorescence quantum yield was observed with increasing dendrimer generation. This is in contrast to results from polyphenylene-dendronized perylenes, for which the fluorescence quantum yield decreased from 0.83 for the first-generation dendrimer down to 0.73 for the third-generation dendrimer.[7b] New nonradiative deactivation pathways were suggested in this case, which do not seem to apply to a pyrene core.

Additional proof for efficient shielding of the core was obtained by fluorescence quenching experiments with nitromethane and *N*,*N*-dimethylaniline. Note that K_{SV} values can only be compared with each other when the fluorescence lifetimes of the investigated fluorophores are equal [Eq. (1)]. Since detailed photophysical investigations were not within the scope of this paper, fluorescence lifetimes of the herein-described dendrimers will be reported in a future paper. However, for polyphenylene dendrimers with perylene diimide as core, fluorescence lifetimes $\langle\tau\rangle_0$ were constant for different sizes of the dendritic shell.[34] It can therefore be assumed that the dendrimers with pyrene as core will also have constant fluorescence lifetimes irrespective of generation. The K_{SV} values significantly decreased on going from TPP to first-generation dendrimer **6** and to second-generation dendrimer **11a**. Remarkably, K_{SV} did not further decrease for the third- and fourth-generation dendrimers. This quenching behavior can not be ascribed only to smaller diffusion constants of the larger dendrimers, since in that case K_{SV} would constantly decrease with increasing generation. Therefore, one can suggest that the second-generation dendrons of **11a** already produced the maximum achievable steric shielding. The K_{SV} values for nitromethane were much larger than those of *N*,*N*-dimethylaniline. For both quenchers almost equal k_q values were reported.[35] It can thus be suggested, that the different quenching behavior originates from a size-exclusion effect provided by the polyphenylene shell, which hampers diffusion of the larger quencher *N*,*N*-dimethylaniline. Tetrachloromethane as fluorescence quencher showed a further strong decrease in K_{SV} between dendrimers **20** and **21**, probably due to an enhanced density of phenyl rings in the outer shell of fourth-generation dendrimer **21**. This suggestion is somewhat confirmed by the fact that steric congestion prevents defect-free growth of a fifth-generation polyphenylene dendrimer when branching unit **8** is used.[36]

In concentrated solutions ($c > 10^{-4}$ M) first-generation dendrimer **10** displayed aggregation of the pyrene core, which suggests that a first-generation polyphenylene shell is too small to inhibit aggregation (Figure 3a). Surprisingly, temperature-dependent fluorescence spectroscopy showed that, even at high temperatures, a 10^{-2} M solution of the first-generation dendrimer still displayed mainly aggregation. A higher temperature is normally expected to hamper self-association due to increased rotational motion of the dendrons within the molecules. However, the small increase in intensity of the absorption band at 440 nm indicated that at lower concentration ($c < 10^{-2}$ M) **10** exists exclusively in the unassociated form at high temperature. Under the same conditions second-generation dendrimer **11a** displayed no aggregation of the core, and this can again be attributed to the larger diameter of the dendritic polyphenylene shell in the case of **11a** (**10**: $d = 2.5$ nm, **11a**: $d = 3.9$ nm).[37] This supports the results derived from the quenching experiments. Moreover, the small influence of temperature on the monomer–aggregate equilibrium of dendronized pyrenes suggested a stiff, temperature-independent arrangement of the dendritic shell. This conclusion is confirmed by investigations on polyphenylene dendrimers by small-angle neutron scattering and solid-state NMR spectroscopy.[6c,d] In the latter case the slowed motion of the terminal phenyl groups was proven and, furthermore, it was demonstrated that the dendrons can not reorient even at high temperatures.

Alkali-metal reduction of second- and fourth-generation dendrimers **11a** and **21** produced the radical anion of the pyrene core. However, significant differences were observed during the reduction of the two dendrimers. With second-generation dendrimer **11a** the radical anion of pyrene was formed immediately, as indicated by UV/Vis and EPR spectroscopy. On the contrary, in the case of fourth-generation dendrimer **21** an intense sharp signal in the EPR spectrum appeared at the beginning. The same sharp signal was observed for reduction of polyphenylene dendrimer **7** without a pyrene core under the same conditions. This leads to the conclusion that charging of the polyphenylene shell of **7** and **21** immediately took place on contact with the potassium mirror. The sharp EPR signal indicated a highly mobile electron spin, which might be due to hopping between different oligomeric phenylene sites. Thus, no specific charged bi- or triphenyl units could be identified.[38] After compro-

portionation with neutral compound, the pyrene radical anion of **21** was also detected. This suggests that a more highly charged state was generated in the beginning, since only in this case does comproportionation result in the radical anion. The observed differences in reduction between **11a** and **21** can be attributed to the larger diameter of fourth-generation dendrimer **21** (**21**: $d=6.8$ nm, **11a**: $d=3.9$ nm).[37] This hampered diffusion of electrons to the pyrene core to such an extent that in the beginning only the charged polyphenylene shell was detected by EPR spectroscopy. On the contrary, for **11a** diffusion of electrons to the core is easier due to the smaller distance between core and outer dendritic shell; thus, the pyrene radical anion could immediately be observed. A diffusion-controlled reduction process can therefore be suggested, strongly influenced by the density and diameter of the surrounding dendrimer shell.

Since good film-forming ability is a major prerequisite for compounds suitable for application in OLEDs, the optical properties of films prepared from alkyl-decorated second-generation dendrimer **11b** were investigated. Films of good quality and high transparency were obtained by simple drop casting and spin coating. Small bathochromic shifts of the emission maximum compared to solution spectra showed that the emission in the film mainly occurred from unaggregated species. Hence, the second-generation dendrons already suppress aggregation of pyrene, not only in solution but also in film.

Conclusion

A series of monodisperse polyphenylene dendrimers with an encapsulated pyrene core has been prepared in high yield by a straightforward divergent growth method. Stern–Volmer quenching experiments and temperature-dependent fluorescence spectroscopy indicated that a second-generation dendrimer shell is sufficient for efficiently shielding the pyrene core and thereby preventing aggregate formation. Alkali-metal reduction of pyrene dendrimers yielded the corresponding pyrene radical anions. Thereby, hampered electron transfer to the core was observed with increasing dendrimer generation, which further verifies the site-isolation concept. From the synthetic point of view, it is interesting that the improvements in the optical properties, such as high quantum efficiency in solution ($Q_f>0.92$), were already achieved by applying a second-generation dendrimer shell, and therefore gram-scale synthesis of these new materials is possible.

The herein-presented macromolecules are exciting new materials that combine excellent optical features and an improved film-forming ability. Thus, application in OLEDs can be suggested and further exploration into this area is underway.

Experimental Section

General procedures: All starting materials, e.g., pyrene (**1**) and tetraphenylcyclopentadienone (**5**), were obtained from commercial suppliers (Aldrich, Fluka, Fischer, Strem, Acros) and were used without purification. Solvents were used in HPLC grade as purchased. All atmosphere-sensitive reactions were performed under argon using Schlenck techniques. ^{1}H and ^{13}C NMR spectra were recorded on a Bruker AMX250, AC300, AMX500, or 700Ultrashield NMR spectrometer. Specific protons in the dendritic structures (positions shown in Scheme 2) are assigned as H_{G1}, H_{G2}, etc. for the corresponding dendrimer generation to which they belong. FD mass spectra were recorded with a VG-Instruments ZAB 2-SE-FDP. MALDI-TOF mass spectra were measured with a Bruker Reflex II and dithranol as matrix (molar ratio dithranol/sample 250:1). UV/Vis absorption spectra were recorded on a Perkin-Elmer Lambda 9 spectrophotometer, and fluorescence spectra on a SPEX Fluorolog II (212) spectrometer. For the temperature-dependent fluorescence measurements an Oxford cryostat (GF 1204) with sapphire windows was used. EPR spectra were recorded on a CW X-band ESP 300 equipped with an NMR gauss meter (Bruker ER 035), a frequency counter (Bruker ER 041 XK), and a variable-temperature continuous-flow N_2 cryostat (Bruker B-VT 2000). Elemental analysis was carried out by the Microanalytical Laboratory of the University of Mainz, Mainz, Germany. Because of the high carbon content in some molecules, incomplete combustion (sooting) may have resulted in lower values than expected for the carbon content. The crystal structure determinations were carried out in glass capillaries on a Nonius KCCD diffractometer with graphite-monochromated $Mo_{K\alpha}$ radiation at 120 K. The structures were solved by direct methods (SHELXS97). Refinement was done with anisotropic temperatures factors for C, and the hydrogen atoms were refined with fixed isotropic temperature factors in the riding mode.

General procedure for the Diels–Alder cycloaddition of ethynyl compounds and tetraphenylcyclopentadiene derivatives: A mixture of the ethynyl compound and tetraphenylcyclopentadienone derivative was refluxed in *o*-xylene or diphenyl ether under argon atmosphere. In the case of the unsubstituted dendrimers, the cooled reaction mixture was poured into pentane to remove the excess of tetraphenylcyclopentadienone. The precipitated product was filtered and the filter washed with pentane until the filtrate became colorless. All crude products were purified by column chromatography (silica gel, petroleum ether/CH_2Cl_2). Reactions were conveniently monitored by MALDI-TOF mass spectrometry to ensure their completeness.

General procedure for the desilylation of triisopropylsilylethynyl derivatives: The triisopropylsilylethynyl derivative was dissolved in dry THF and 1 equiv of TBAF (dissolved in THF) per triisopropylsilylethynyl group was added under argon atmosphere. The end of the reaction (ca. 5–15 min) was determined by TLC. The reaction was quenched with water, and the reaction mixture extracted with water and CH_2Cl_2. The organic phase was separated and dried over $MgSO_4$. After having removed the solvent under reduced pressure, the crude product was purified by column chromatography (silica gel, petroleum ether/CH_2Cl_2).

1,3,6,8-Tetrabromopyrene (2): Pyrene (0.5 g, 2.47 mmol) was dissolved in nitrobenzene (15 mL). Under vigorous stirring, bromine (1.62 g, 10.13 mmol) was added. After complete addition, the temperature was increased to 160 °C and maintained for 3 h. The cooled reaction suspension was poured into acetone and the precipitate filtered off. Further drying of the precipitate in high vacuum gave the crude product, which was used without further purification (1.15 g, 2.22 mmol, 90 %). ^{1}H NMR (500 MHz, [D_5]nitrobenzene, 433 K, TMS): $\delta=8.44$ (s, 2H; 2,7-pyrene H), 8.42 ppm (s, 4H; 4,5,9,10-pyrene H); MS (FD, 8 kV): m/z (%): 517.98 (100) $[M]^+$.

1,3,6,8-Tetrakis(trimethylsilanylethynyl)pyrene (3): Compound **2** (0.5 g, 0.97 mmol) was suspended in triethylamine (20 mL) and toluene (3 mL), and bis(triphenylphosphine)palladium(II) dichloride (136 mg, 0.19 mmol), copper(I) iodide (73 mg, 0.39 mmol), and triphenylphosphine (101 mg, 0.39 mmol) were added. The flask was evacuated and flushed with argon. While stirring, the reaction mixture was heated to 60 °C and trimethylsilylethyne (0.57 g, 5.8 mmol) was injected through a septum. After 15 min

of stirring at this temperature the reaction was heated to 80 °C and stirred overnight under argon atmosphere. The cooled reaction mixture was diluted with CH_2Cl_2 and extracted with water. The organic phase was dried over $MgSO_4$, and the solvent was removed under reduced pressure. The crude product was purified by column chromatography (silica gel, petroleum ether) to afford **3** as an orange solid (470 mg, 0.8 mmol, 83 %). ^{1}H NMR (250 MHz, CD_2Cl_2, 300 K, TMS): $\delta = 8.59$ (m, 4H; 4,5,9,10-pyrene H), 8.27 (s, 2H; 2,7-pyrene H), 0.39 ppm (s, 36H; CH_3); ^{13}C NMR (75 MHz, CD_2Cl_2, 300 K, TMS): $\delta = 134.7$, 132.3, 127.3, 123.8, 119.1 (all aromat. C), 102.8 (Ar−*C*≡C), 102.1 (≡C−Si), 0.1 ppm (CH_3); MS (FD, 8 kV): *m*/*z* (%): 587.24 (100) $[M]^+$; elemental analysis calcd (%) for $C_{36}H_{42}Si_4$: C 73.65, H 7.21; found: C 73.14, H 7.55.

1,3,6,8-Tetraethynylpyrene (4): Compound **3** (1 g, 1.7 mmol) was suspended in methanol (100 mL). K_2CO_3 (1.9 g, 13.6 mmol) was added and the reaction mixture stirred overnight and then poured into water (500 mL) and filtered. The filter was washed with water until the filtrate was neutral to afford **4** as a slightly brown solid (480 mg, 1.61 mmol, 95 %). ^{1}H NMR (300 MHz, [D$_8$]THF, 300 K, TMS): $\delta = 8.70$ (s, 4H; 4,5,8,10-pyrene H), 8.36 (s, 2H; 2,7-pyrene H), 4.31 ppm (s, 4H; ≡CH); ^{13}C NMR (75 MHz, [D$_8$]THF, 300 K, TMS): $\delta = 135.6$, 133.1, 127.7, 124.4, 119.2 (all aromat. C), 86.2 (Ar−C≡C), 81.8 ppm (≡CH); MS (FD, 8 kV): *m*/*z* (%): 298.08 (100) $[M]^+$.

Compound 6: Compounds **4** (0.2 g, 0.67 mmol) and **5** (1.55 g, 4.03 mmol) were heated in *o*-xylene (20 mL) for 12 h at 160 °C. The reaction mixture was poured into methanol and the precipitate filtered off. Compound **6** was obtained by repeated precipitation from ethanol (1.08 g, 0.63 mmol, 95 %) until the red color of **5** had disappeared. ^{1}H NMR (700 MHz, $C_2D_2Cl_4$, 373 K, TMS): $\delta = 7.86$–7.40 (m, 6H; pyrene H), 7.24–6.52 ppm (m, 84H; aromat. H); ^{13}C NMR (75 MHz, CD_2Cl_2, 300 K, TMS): $\delta =$ 142.1, 141.7, 141.1, 141.0, 140.7, 140.5, 140.3, 139.9, 131.9, 131.8, 131.3, 131.0, 130.3, 128.3, 128.2, 128.1, 127.4, 127.5, 126.9, 126.6, 126.4, 126.2, 125.6, 125.3, 125.2, 125.1 ppm (all aromat. C); MS (FD, 8 kV): *m*/*z* (%): 1725 (100) $[M]^+$.

Compound 9: Compounds **4** (250 mg, 0.84 mmol) and **8** (3.0 g, 4.03 mmol) were heated in *o*-xylene (30 mL) for 12 h at 160 °C. Purification was performed by column chromatography (silica gel, petroleum ether/CH_2Cl_2) to afford **9** as a yellow solid (1.88 g, 0.59 mmol, 71 %). ^{1}H NMR (250 MHz, CD_2Cl_2, 300 K, TMS): $\delta = 8.02$–7.57 (m, 6H; pyrene H), 7.42 (m, 4H; H_{G1}), 7.19–6.61 (m, 72H; aromat. H), 1.10 ppm (s, 215H; CH/CH_3); ^{13}C NMR (75 MHz, [D$_8$]THF, 300 K, TMS): $\delta = 142.3$, 142.2, 141.9, 141.9, 141.8, 141.7, 141.7, 141.6, 141.6, 141.6, 141.6, 141.5, 141.5, 141.4, 141.3, 141.3, 141.2, 141.1, 140.9, 140.9, 140.7, 140.6, 140.5, 140.4, 140.4, 139.9, 139.6, 139.6, 139.5, 139.4, 139.4, 139.3, 137.4, 137.3, 137.2, 137.1, 136.8, 136.5, 136.0, 132.4, 132.4, 131.6, 131.3, 130.7, 130.6, 130.7, 129.7, 129.0, 128.9, 128.8, 128.7, 128.4, 128.0, 127.5, 127.2, 126.5, 126.0, 125.2, 121.7, 121.4 (all aromat. C), 108.5 (Ar−*C*≡), 90.2, 90.0 (both ≡C−Si), 19.0 (CH_3), 12.2 ppm (CH); MALDI-TOF-MS: *m*/*z* (%): 3166 (100) $[M]^+$.

Compound 10: Compound **9** (1.43 g, 0.45 mmol) was dissolved in dry THF (30 mL) and treated with TBAF (1.14 g, 3.6 mmol). Purification was performed by column chromatography (silica gel, petroleum ether/CH_2Cl_2) to afford **10** as a yellow solid (0.8 g, 0.42 mmol, 93 %). ^{1}H NMR (250 MHz, CD_2Cl_2, 300 K, TMS): $\delta = 7.89$–7.73 (m, 6H; pyrene H), 7.53–7.43 (m, 4H; H_{G1}), 7.17–6.60 (m, 80H; aromat. H), 3.02 ppm (m, 8H; ≡CH); ^{13}C NMR (75 MHz, [D$_8$]THF, 300 K, TMS): $\delta = 142.3$, 142.2, 142.1, 141.9, 141.8, 141.7, 141.6, 141.6, 141.5, 141.5, 141.3, 141.3, 141.2, 141.2, 141.1, 140.9, 140.8, 140.7, 140.6, 140.6, 140.5, 140.4, 140.3, 140.2, 139.9, 139.6, 139.5, 139.5, 139.4, 139.4, 139.3, 137.3, 137.3, 137.3, 137.1, 136.9, 136.8, 136.5, 136.4, 136.1, 134.8, 134.6, 134.4, 134.2, 133.9, 132.7, 132.5, 132.3, 131.9, 131.6, 131.3, 130.7, 130.6, 130.1, 129.6, 128.9, 128.9, 128.7, 128.5, 128.1, 127.5, 127.3, 126.8, 126.5, 126.5, 126.3, 126.1, 126.0, 125.9, 125.5, 125.4, 125.2, 125.1, 125.0, 121.0, 120.6 (all aromat. C), 84.2 (Ar−*C*≡), 78.7, 78.6 (both ≡CH), 67.4 ppm (C_q); MALDI-TOF-MS: *m*/*z* (%): 1916 (100) $[M]^+$; elemental analysis calcd (%) for $C_{152}H_{90}$: C 95.27, H 4.73; found C 94.61, H 4.91.

Compound 11a: Compounds **10** (200 mg, 0.1 mmol) and **5** (640 mg, 1.67 mmol) were dissolved in *o*-xylene (10 mL) and heated for 16 h at 160 °C. Purification was performed by column chromatography (silica gel, petroleum ether/CH_2Cl_2) to afford **11** as a yellow solid (360 mg, 76 μmol, 73 %. ^{1}H NMR (250 MHz, CD_2Cl_2, 300 K, TMS): $\delta = 7.78$–7.61 (m, 6H; pyrene H), 7.43–7.35 (m, 12H; H_{G1+G2}), 7.16–6.53 ppm (m, 232H; aromat. H); ^{13}C NMR (75 MHz, [D$_8$]THF, 300 K, TMS): $\delta = 142.8$, 142.7, 142.0, 141.7, 141.4, 141.3, 141.1, 141.0, 140.1, 140.1, 140.0, 139.7, 139.4, 139.2, 138.9, 132.4, 132.0, 130.6, 129.5, 129.2, 129.1, 128.3, 127.6, 127.3, 126.9, 126.3, 126.0 ppm (all aromat. C); MALDI-TOF-MS: *m*/*z* (%): 4768 (100) $[M]^+$; elemental analysis calcd (%) for $C_{376}H_{250}$: C 94.72, H 5.87; found C 94.00, H 5.87.

Compound 11b: Compounds **10** (18 mg, 9.4 μmol) and **14** (140 mg, 132 μmol) were dissolved in Ph_2O (4 mL) and heated for 16 h at 220 °C. Purification was performed by column chromatography (silica gel, petroleum ether/CH_2Cl_2) to afford **11b** as a yellow oil (60 mg, 5.9 μmol, 63 %). ^{1}H NMR (500 MHz, CD_2Cl_2, 300 K, TMS): $\delta = 7.80$–6.42 (m, 234H; aromat. H), 2.31 (m, 16H; CH), 1.27–1.19 (m, 672H; CH_2), 0.88–0.87 ppm (m, 96H; CH_3); ^{13}C NMR (125 MHz, CD_2Cl_2, 300 K, TMS): $\delta =$ 168.2, 168.0, 156.9, 156.3, 142.8, 142.7, 142.5, 141.9, 141.7, 141.4, 141.4, 141.2, 141.0, 140.9, 140.9, 140.8, 140.2, 140.1, 139.9, 139.8, 139.6, 139.4, 139.3, 138.9, 138.7, 138.7, 138.5, 138.2, 135.6, 134.3, 133.9, 133.6, 133.3, 133.2, 133.0, 132.8, 132.3, 131.9, 131.8, 131.7, 131.5, 131.4, 131.4, 131.1, 130.7, 130.6, 130.4, 130.4, 130.3, 130.3, 130.2, 130.0, 129.9, 129.8, 129.5, 129.4, 129.3, 129.3, 129.2, 129.0, 128.9, 128.7, 128.6, 128.5, 128.4, 128.2, 128.0, 128.0, 127.9, 127.7, 127.6, 127.4, 126.6, 126.0, 125.6, 120.5 (all aromat. C), 41.21, 40.77, 40.63, 40.22, 40.19, 39.71, 39.64, 39.51, 39.44 (all αCH$_2$/CH), 33.71, 33.62, 34.17, 34.00, 32.52, 30.65, 30.29, 30.25, 29.92, 27.10, 27.13, 23.23 (all CH_2), 14.33 ppm (CH_3); MALDI-TOF-MS: *m*/*z* (%): 10161 (100) $[M]^+$.

1,2-Bis[4-(2-decyltetradecyl)phenyl]ethane-1,2-dione (13): Compound **12** (2.2 g, 2.58 mmol) and iodine (330 mg, 1.3 mmol) were dissolved in DMSO (30 mL). The mixture was stirred for 24 h at 170 °C and the product extracted with CH_2Cl_2 and water. The organic phase was removed in vacuo and the residue was purified by column chromatography (silica gel, hexane/ethyl acetate) to give **13** as a colorless oil (0.9 g, 1.0 mmol, 40 %). ^{1}H NMR (300 MHz, CD_2Cl_2, 300 K, TMS): $\delta = 7.86$ (d, ^3J(H,H) = 8.3 Hz, 4H; 2,2′,6,6′-aromat. H), 7.31 (d, ^3J(H,H) = 8.3 Hz, 4H; 3,3′,5,5′-aromat. H), 2.62 (d, ^3J(H,H) = 7.0 Hz, 4H; αCH$_2$), 1.66 (m, 2H; CH), 1.50–1.10 (m, 80H; CH_2), 0.89 ppm (t, ^3J(H,H) = 6.5 Hz, 12H; CH_3); ^{13}C NMR (75 MHz, CD_2Cl_2, 300 K, TMS): $\delta = 195.0$ (C=O), 150.8 (4,4′-aromat. C), 131.2 (2,2′,6,6′-aromat. C), 130.2 (3,3′,5,5′-aromat. C), 130.1 (1,1′-aromat. C), 41.2 (αCH$_2$), 40.0 (CH), 33.5, 32.4, 30.3, 30.1, 29.8, 26.9, 23.1 (all CH_2), 14.3 ppm (CH_3); MS (FD, 8 kV): *m*/*z* (%): 441.8 (100) $[M]^{2+}$, 883.6 (45) $[M]^+$.

3,4-Bis[4-(2-dodecyltetradecyl)phenyl]-2,5-diphenyl-cyclopenta-2,4-dienone (14): Compound **13** (1.37 g, 1.55 mmol) and 1,3-diphenylpropan-2-one (326 mg, 1.55 mmol) were dissolved in degassed *t*BuOH (3 mL) at 80 °C. 1 mL of a 0.8 M solution of tetrabutylammonium hydroxide in methanol was diluted with *t*BuOH (3 mL) and added to the reaction mixture. After 20 min the reaction was stopped by adding water (10 mL). Extraction with CH_2Cl_2 and concentration of the organic layer gave a residue which was further purified by column chromatography to obtain **14** as a purple oil (802 mg, 0.76 mmol, 49 %). ^{1}H NMR (300 MHz, CD_2Cl_2, 300 K, TMS): $\delta = 7.23$ (s, 10H; aromat. H), 6.95 (d, ^3J(H,H) = 8.2 Hz, 4H; aromat. H), 6.8 (d, ^3J(H,H) = 8.2 Hz, 4H; aromat. H), 2.47 (d, 4H; αCH$_2$), 1.40–1.10 (m, 80H; CH_2), 0.88 ppm (t, ^3J(H,H) = 6.9 Hz, 12H; CH_3); ^{13}C NMR (75 MHz, CD_2Cl_2, 300 K, TMS): $\delta = 200.8$ (C=O), 155.4, 143.2, 131.7, 130.8, 130.5, 129.6, 129.0, 128.3, 127.6, 125.3 (all aromat. C), 40.9 (αCH$_2$), 40.0 (CH), 33.6, 32.3, 30.4, 30.1, 30.1, 29.8, 26.9, 23.1 (all CH_2), 14.3 ppm (CH_3); MS (FD, 8 kV): *m*/*z* (%): 1058.2 (100) $[M]^+$.

Compound 15: Compounds **10** (300 mg, 0.16 mmol) and **8** (1.4 g, 1.88 mmol) were dissolved in *o*-xylene (10 mL) and heated for 20 h at 150 °C. Purification was performed by column chromatography (silica gel, petroleum ether/CH_2Cl_2) to afford **15** as a yellow solid (0.91 g, 0.12 mmol, 76 %). ^{1}H NMR (250 MHz, CD_2Cl_2, 300 K, TMS): $\delta = 7.78$–7.61 (m, 6H; pyrene H), 7.42–7.31 (m, 12H; H_{G1+G2}), 7.18–6.40 (m, 216H; aromat. H), 1.09 ppm (s, 336H; CH/CH_3); ^{13}C NMR (75 MHz, [D$_8$]THF, 300 K, TMS): $\delta = 142.6$, 142.4, 141.9, 141.9, 141.8, 141.7, 141.4, 141.2, 141.0, 140.6, 140.5, 140.4, 140.3, 140.1, 140.0, 139.6, 139.5, 139.2, 139.2, 138.9, 137.4, 136.9, 136.6, 136.2, 132.3, 131.5, 131.2, 130.8, 130.6,

130.1, 129.5, 129.2, 128.8, 128.5, 128.3, 127.8, 127.2, 127.0, 126.7, 126.7, 126.5, 123.8, 121.6, 121.3 (all aromat. C), 108.5, 108.5 (both Ar−*C*≡), 90.2, 90.0 (both ≡C−Si), 67.4 (C_q), 19.0 (CH_3), 12.2 ppm (CH); MALDI-TOF-MS: *m*/*z* (%): 7657 (100) $[M]^+$; elemental analysis calcd (%) for $C_{552}H_{570}Si_{16}$: C 86.62, H 7.51; found C 86.94, H 7.61.

Compound 16: Compound **15** (0.8 g, 0.1 mmol) was dissolved in dry THF (15 mL) and treated with TBAF (518 mg, 1.67 mmol). Purification was performed by column chromatography (silica gel, petroleum ether/CH_2Cl_2) to afford **16** as a yellow solid (0.49 g, 95 μmol, 91 %). ^{1}H NMR (250 MHz, CD_2Cl_2, 300 K, TMS): δ = 7.78–7.61 (m, 6H; pyrene H), 7.46–7.32 (m, 12H; H_{G1+G2}), 7.18–6.54 (m, 216H; aromat. H), 3.02 ppm (m, 16H; ≡CH); ^{13}C NMR (75 MHz, [D$_8$]THF, 300 K, TMS): δ = 141.6, 141.3, 141.1, 139.5, 139.4, 139.0, 138.8, 138.5, 131.8, 131.5, 131.2, 130.8, 130.2, 129.0, 128.6, 128.1, 127.9, 127.4, 126.9, 126.2, 119.7, 119.4 (all aromat. C), 83.8 (Ar−*C*≡), 77.3 ppm (≡CH); MALDI-TOF-MS; *m*/*z* (%): 5147 (100) $[M]^+$; elemental analysis calcd (%) for $C_{408}H_{250}$: C 95.11, H 4.89; found C 94.38, H 5.76.

Compound 17: Compounds **16** (200 mg, 39 μmol) and **8** (0.93 g, 1.25 mmol) were dissolved in *o*-xylene (10 mL) and heated for 20 h at 160 °C. Purification was performed by column chromatography (silica gel, petroleum ether/CH_2Cl_2) to afford **17** as a yellow solid (0.55 g, 33 μmol, 85 %). ^{1}H NMR (250 MHz, CD_2Cl_2, 300 K, TMS): δ = 7.78–7.59 (m, 6H; pyrene H), 7.40–7.27 (m, 28H; $H_{G1–G3}$), 7.17–6.38 (m, 504H; aromat. H), 1.08 ppm (s, 672H; CH/CH_3); ^{13}C NMR (75 MHz, [D$_8$]THF, 300 K, TMS): δ = 142.8, 142.7, 142.7, 142.4, 141.9, 141.9, 141.8, 141.7, 141.4, 141.0, 140.9, 140.6, 140.1, 140.0, 139.9, 139.8, 139.5, 139.3, 139.2, 139.2, 139.1, 139.0, 138.8, 137.4, 136.9, 132.3, 132.0, 131.5, 131.2, 130.7, 130.6, 130.1, 129.4, 129.1, 128.5, 128.3, 127.8, 127.2, 126.9, 126.7, 126.5, 121.6, 121.3 (all aromat. C), 108.5 (Ar−*C*≡), 90.2, 90.0 (both ≡CH), 19.0 (CH_3), 12.2 ppm (CH); MALDI-TOF-MS: *m*/*z* (%): 16640 (100) $[M]^+$; elemental analysis calcd (%) for $C_{1208}H_{1210}Si_{32}$: C 87.26, H 7.33; found C 86.22, H 7.79.

Compound 18: Compound **17** (0.4 g, 24.1 μmol) was dissolved in dry THF (15 mL) and treated with TBAF (243 mg, 0.77 mmol). Purification was performed by column chromatography (silica gel, petroleum ether/CH_2Cl_2) to afford **18** as a yellow solid (250 mg, 21.5 μmol, 89 %). ^{1}H NMR (250 MHz, CD_2Cl_2, 300 K, TMS): δ = 7.77–7.59 (m, 6H; pyrene H), 7.42 (m, 8H; H_{G2}), 7.38 (m, 16H; H_{G3}), 7.31–7.29 (m, 4H; H_{G1}), 7.13–6.44 (m, 504H; aromat. H), 3.04–2.00 ppm (m, 32H; ≡CH); ^{13}C NMR (75 MHz, [D$_8$]THF, 300 K, TMS): δ = 142.8, 142.7, 142.3, 141.9, 141.8, 141.8, 141.7, 141.4, 141.0, 140.9, 140.5, 140.0, 139.9, 139.4, 139.3, 139.2, 139.2, 139.0, 138.8, 132.4, 132.0, 131.5, 131.2, 130.7, 130.6, 129.4, 129.1, 128.5, 128.3, 127.8, 127.2, 127.0, 126.9, 126.7, 126.5, 120.9, 120.6 (all aromat. C), 84.2 (Ar−*C*≡), 78.6 ppm (≡CH); MALDI-TOF-MS: *m*/*z* (%): 11618 (100) $[M]^+$.

Compound 20: Compounds **10** (100 mg, 52 μmol) and **19** (950 mg, 0.83 mmol) were dissolved in *o*-xylene (10 mL) and heated for 2 d at 170 °C. The solvent was removed under reduced pressure and the crude product was purified by column chromatography (silica gel, petroleum ether/CH_2Cl_2) to afford **20** as a yellow solid (310 mg, 29 μmol, 55 %). ^{1}H NMR (250 MHz, CD_2Cl_2, 300 K, TMS): δ = 7.76–7.60 (m, 6H; pyrene H), 7.41 (m, 8H; H_{G2}), 7.37 (m, 16H; H_{G3}), 7.32–7.29 (m, 4H; H_{G1}), 7.13–6.44 ppm (m, 536H; aromat. H); ^{13}C NMR (75 MHz, [D$_8$]THF, 300 K, TMS): δ = 142.8, 142.7, 142.0, 141.7, 141.4, 141.4, 141.3, 141.1, 141.0, 140.2, 140.1, 140.0, 140.0, 139.7, 139.5, 139.4, 139.4, 139.2, 138.9, 132.4, 132.0, 130.6, 129.6, 129.5, 129.2, 128.9, 128.3, 127.6, 127.3, 126.9, 126.5, 126.3, 126.3, 126.0 ppm (all aromat. C); MALDI-TOF-MS: *m*/*z* (%): 10837 (100) $[M]^+$; elemental analysis calcd (%) for $C_{856}H_{570}$: C 94.71, H 5.29; found C 94.50, H 5.24.

Compound 21: Compounds **18** (100 mg, 8.6 μmol) and **5** (420 mg, 0.56 mmol) were dissolved in Ph_2O (8 mL) and heated for 5 d at 190 °C. Purification was performed by column chromatography (silica gel, petroleum ether/CH_2Cl_2) to afford **21** as a yellow solid (170 mg, 7.3 μmol, 85 %). ^{1}H NMR (250 MHz, CD_2Cl_2, 300 K, TMS): δ = 7.79–7.59 (m, 6H; pyrene H), 7.41–7.30 (m, 58H; $H_{G1–G4}$), 7.14–6.42 ppm (m, 1146H; aromat. H); ^{13}C NMR (75 MHz, [D$_8$]THF, 300 K, TMS): δ = 142.8, 142.7, 142.0, 141.7, 141.4, 141.3, 141.1, 141.0, 140.1, 140.1, 140.0, 139.7, 139.4, 139.2, 138.9, 132.4, 132.0, 130.6, 129.5, 129.2, 129.1, 128.3, 127.6, 127.3, 126.9, 126.3, 126.0 ppm (all aromat. C); MALDI-TOF-MS: *m*/*z* (%): 23019 (100) $[M]^+$; elemental analysis calcd (%) for $C_{1816}H_{1210}$: C 94.70, H 5.30; found C 94.58, H 5.37.

1,3,6,8-Tetrakis(phenylethynyl)pyrene (22): Compound **2** (314 mg, 61 μmol) was suspended in triethylamine (15 mL) and toluene (5 mL), and bis(triphenylphosphine)palladium(II) dichloride (130 mg, 0.18 mmol), copper(I) iodide (45 mg, 0.24 mmol), and triphenylphosphine (64 mg, 0.24 mmol) were added. The flask was evacuated and flushed with argon. Under stirring, the reaction mixture was heated to 60 °C and phenylacetylene (0.56 mL, 4.8 mmol) was injected through a septum. After 15 min of stirring the reaction was heated to 80 °C and stirred overnight under argon atmosphere. After cooling, the reaction mixture was filtered and the orange precipitate **22** thoroughly washed with CH_2Cl_2 and acetone (340 mg, 56.4 μmol, 92 %). ^{1}H NMR (250 MHz, CD_2Cl_2, 300 K, TMS): δ = 7.78–7.69 (m, 6H; pyrene H), 7.56–7.02 ppm (m, 20H; aromat. H); ^{13}C NMR (125 MHz, $C_2D_2Cl_4$, 373 K, TMS): δ = 134.1 (1,3,6,8-pyrene C), 132.2, 132.1, 128.9, 128.7 (all aromat. C), 127.2 (2,7-pyrene C), 124.5, 123.6 (both aromat. C), 119.5 (4,5,9,10-pyrene C), 96.8 (Ar−*C*≡), 88.1 ppm (pyrene −C≡); MS (FD, 8 kV): *m*/*z* (%): 603.1 (100) $[M]^+$, 301.7 (20) $[M]^{2+}$.

Compound 23: Compounds **22** (79 mg, 0.13 mmol) and **5** (300 mg, 0.78 mmol) were dissolved in Ph_2O (5 mL) and heated for 24 h at 230 °C. Purification was performed by column chromatography (silica gel, petroleum ether/CH_2Cl_2) to afford **23** as a yellow solid (170 mg, 7.3 μmol, 90 %). ^{1}H NMR (500 MHz, $C_2D_2Cl_4$, 373 K, TMS): δ = 7.31 (d, ^3J(H,H) = 6.0 Hz, 2H; 2,7-pyrene H), 7.23 (d, ^3J(H,H) = 5.5 Hz, 4H; 4,5,9,10-pyrene H), 6.81–6.75 (m, 80H; aromat. H), 6.52 ppm (m, 20H; aromat. H); ^{13}C NMR (500 MHz, $C_2D_2Cl_4$, 373 K, TMS): δ = 141.6, 141.3, 140.8, 140.7, 138.6, 134.8, 134.0, 131.9, 131.8, 131.4, 126.6, 126.5, 126.3, 125.1, 125.0 ppm (all aromat. C); MS (FD, 8 kV): *m*/*z* (%): 2031.4 (100) $[M]^+$.

Acknowledgements

Financial support by the Deutsche Forschungsgemeinschaft (SFB 625) is gratefully acknowledged. We thank C. Beer for synthetic support.

[1] a) I. Carmichael, G. L. Hug, *Handbook of Photochemistry*, 2nd ed., Marcel Dekker, New York, **1993**; b) J. B. Birks, *Photophysics of Aromatic Molecules*, Wiley Interscience, London, **1970**.

[2] a) E. M. S. Castanheira, J. M. G. Martinho, *Chem. Phys. Lett.* **1991**, *185*, 319–323; b) D. C. Dong, M. A. Winnik, *Can. J. Chem.* **1984**, *62*, 2560–2565.

[3] A. Thomas, S. Polarz, M. Antonietti, *J. Phys. Chem. B* **2003**, *107*, 5081–5087.

[4] a) C. M. Cardona, T. Wilkes, W. Ong, A. E. Kaifer, T. D. McCarley, S. Pandey, G. A. Baker, M. N. Kane, S. N. Baker, F. V. Bright, *J. Phys. Chem. B* **2002**, *106*, 8649–8656; b) S. Hecht, N. Vladimirov, J. M. J. Fréchet, *J. Am. Chem. Soc.* **2001**, *123*, 18–25; c) L. A. Baker, R. M. Crooks, *Macromolecules* **2000**, *33*, 9034–9039; d) R. Wilken, J. Adams, *Macromol. Rapid Commun.* **1997**, *18*, 659–665.

[5] For OLEDs in general see, for example: a) A. P. Kulkarni, C. J. Tonzola, A. Babel, S. A. Jenekhe, *Chem. Mater.* **2004**, *16*, 4556–4573; b) L. S. Hung, C. H. Chen, *Mater. Sci. Eng. R* **2002**, *39*, 143–222; c) M. T. Bernius, M. Inbasekaran, J. O'Brien, W. S. Wu, *Adv. Mater.* **2000**, *12*, 1737–1750; d) Y. Cao, I. D. Parker, G. Yu, C. Zhang, A. J. Heeger, *Nature* **1999**, *397*, 414–417. For pyrene containing devices, see: e) W. L. Jia, T. McCormick, Q. D. Liu, H. Fukutani, M. Motala, R. Y. Wang, Y. Tao, S. N. Wang, *J. Mater. Chem.* **2004**, *14*, 3344–3350; f) V. Cimrová, D. Výprachtický, *Appl. Phys. Lett.* **2003**, *82*, 642–644; g) Y. Aso, T. Okai, Y. Kawaguchi, T. Otsubo, *Chem. Lett.* **2001**, 420–421.

[6] a) M. Wind, U. M. Wiesler, K. Saalwächter, K. Müllen, H. W. Spiess, *Adv. Mater.* **2001**, *13*, 752–756; b) H. Zhang, P. C. M. Grim, P. Foubert, T. Vosch, P. Vanoppen, U. M. Wiesler, A. J. Berresheim, K. Müllen, F. C. De Schryver, *Langmuir* **2000**, *16*, 9009–9014; c) S. Rosenfeldt, N. Dingenouts, D. Potschke, M. Ballauff, A. J. Berre-

sheim, K. Müllen, P. Lindner, *Angew. Chem.* **2003**, *115*, 111–114; *Angew. Chem. Int. Ed.* **2004**, *43*, 109–112; d) M. Wind, K. Saalwächter, U. M. Wiesler, K. Müllen, H. W. Spiess, *Macromolecules* **2002**, *35*, 10071–10086.

[7] a) D. J. Liu, S. De Feyter, M. Cotlet, A. Stefan, U. M. Wiesler, A. Herrmann, D. Grebel-Koehler, J. Q. Qu, K. Müllen, F. C. De Schryver, *Macromolecules* **2003**, *36*, 5918–5925; b) A. Herrmann, T. Weil, V. Sinigersky, U. M. Wiesler, T. Vosch, J. Hofkens, F. C. De Schryver, K. Müllen, *Chem. Eur. J.* **2001**, *7*, 4844–4853.

[8] a) J. N. G. Pillow, M. Halim, J. M. Lupton, P. L. Burn, I. D. W. Samuel, *Macromolecules* **1999**, *32*, 5985–5993; b) P. W. Wang, Y. J. Liu, C. Devadoss, P. Bharathi, J. S. Moore, *Adv. Mater.* **1996**, *8*, 237.

[9] J. Q. Qu, D. J. Liu, S. De Feyter, J. Y. Zhang, F. C. De Schryver, K. Müllen, *J. Org. Chem.* **2003**, *68*, 9802–9808.

[10] a) E. M. Harth, S. Hecht, B. Helms, E. E. Malmström, J. M. J. Fréchet, C. J. Hawker, *J. Am. Chem. Soc.* **2002**, *124*, 3926–3938; b) V. Rozhkov, D. Wilson, S. Vinogradov, *Macromolecules* **2002**, *35*, 1991–1993.

[11] C. B. Gorman, J. C. Smith, M. W. Hager, B. L. Parkhurst, H. Sierzputowska-Gracz, C. A. Haney, *J. Am. Chem. Soc.* **1999**, *121*, 9958–9966.

[12] a) K. Ogino, S. Iwashima, H. Inokuchi, Y. Harada, *Bull. Chem. Soc. Jpn.* **1965**, *38*, 473–477; b) Vollmann, *Liebigs Ann. Chem.* **1937**, *531*, 1.

[13] a) Y. F. Wang, W. Deng, L. Liu, Q. X. Guo, *Chin. J. Org. Chem.* **2005**, *25*, 8–24; b) K. Sonogashira, S. Takahashi, *J. Synth. Org. Chem. Jpn.* **1993**, *51*, 1053–1063; c) H. A. Dieck, F. R. Heck, *J. Organomet. Chem.* **1975**, *93*, 259–263.

[14] a) U. M. Wiesler, T. Weil, K. Müllen, *Top. Curr. Chem.* **2001**, *212*, 1–40; b) F. Morgenroth, E. Reuther, K. Müllen, *Angew. Chem.* **1997**, *109*, 647–649; *Angew. Chem. Int. Ed. Engl.* **1997**, *36*, 631–634.

[15] F. Morgenroth, K. Müllen, *Tetrahedron* **1997**, *53*, 15349–15366.

[16] U. M. Wiesler, K. Müllen, *Chem. Commun.* **1999**, 2293–2294.

[17] W. Pisula, M. Kastler, D. Wasserfallen, T. Pakula, K. Müllen, *J. Am. Chem. Soc.* **2004**, *126*, 8074–8075.

[18] R. E. Bauer, V. Enkelmann, U. M. Wiesler, A. J. Berresheim, K. Müllen, *Chem. Eur. J.* **2002**, *8*, 3858–3864.

[19] CCDC-285925 contains the supplementary crystallographic data for this paper. These data can be obtained free of charge from the Cambridge Crystallographic Data Centre via www.ccdc.cam.ac.uk/data_request/cif.

[20] The absorption maxima $\lambda_{max\,abs}$ and emission maxima $\lambda_{max\,em}$ and corresponding molar extinction coefficients ε for unsubstituted pyrene and the dendronized pyrenes are given in the Supporting Information.

[21] I. B. Berlman, *J. Phys. Chem.* **1970**, *74*, 3085–3093.

[22] Extinction coefficients are in line with values reported by others: a) F. M. Winnik, M. A. Winnik, S. Tazuke, C. K. Ober, *Macromolecules* **1987**, *20*, 38–44; b) K. Hara, W. R. Ware, *Chem. Phys.* **1980**, *51*, 61–68.

[23] D. F. Eaton, *Pure Appl. Chem.* **1988**, *60*, 1107–1114. Q_f: 0.90, solvent: cyclohexane, excitation wavelength: 350 nm.

[24] D. C. Dong, M. A. Winnik, *Can. J. Chem.* **1984**, *62*, 2560–2565.

[25] a) M. Stepanek, K. Krijtova, K. Prochazka, Y. Teng, S. E. Webber, P. Munk, *Acta Polym.* **1998**, *49*, 96–102; b) M. Stepanek, K. Krijtova, Z. Limpouchova, K. Prochazka, Y. Teng, P. Munk, S. E. Webber, *Acta Polym.* **1998**, *49*, 103–107.

[26] T. Förster, *Angew. Chem.* **1969**, *81*, 364–374; *Angew. Chem. Int. Ed. Engl.* **1969**, *8*, 333–343.

[27] T. Keeling-Tucker, J. D. Brennan, *Chem. Mater.* **2001**, *13*, 3331–3350.

[28] Compound **10** was chosen instead of **6** due to its better solubility. The peripheral ethynyl groups were not expected to significantly enlarge the dendrimer dimensions. The absorption maxima of **10** and **11a** did not shift with increasing temperature.

[29] a) J. Zhang, R. E. Campbell, A. Y. Ting, R. Y. Tsien, *Nat. Rev. Mol. Cell Biol.* **2002**, *3*, 906–918; b) D. L. Taylor, Y. L. Wang, *Nature* **1980**, *284*, 405–410.

[30] M. Baumgarten, K. Müllen, *Top. Curr. Chem.* **1994**, *169*, 1–103.

[31] K. H. J. Buschow, J. Dieleman, G. J. Hoijtink, *J. Chem. Phys.* **1965**, *42*, 1993–1998.

[32] I. C. Lewis, L. S. Singer, *J. Chem. Phys.* **1965**, *43*, 2712–2727.

[33] For ease of comparison the EPR spectra of **7**, **11a**, and **21** are collected in the Supporting Information.

[34] R. Pilot, E. Fron, F. C. De Schryver, Katholieke Universiteit Leuven (Belgium), personal communication.

[35] Pyrene on the focal point of a first-generation poly(amido) dendrimer.[4a] k_q nitromethane $5.66\pm0.14\times10^9\,M^{-1}s^{-1}$, k_q *N*,*N*-dimethylaniline $6.24\pm0.30\times10^9\,M^{-1}s^{-1}$.

[36] U. M. Wiesler, Dissertation, Johannes Gutenberg Universität Mainz (Germany), **2001**.

[37] Distances were derived from three-dimensional structures calculated by the MMFF method. T. A. Halgren, *J. Comput. Chem.* **1996**, *17*, 490–519.

[38] a) T. Shida, S. Iwata, *J. Am. Chem. Soc.* **1973**, *95*, 3473–3483; b) D. F. Lindow, C. N. Cortez, R. G. Harvey, *J. Am. Chem. Soc.* **1972**, *94*, 5406; c) T. Shida, S. Iwata, *J. Chem. Phys.* **1972**, *56*, 2858; d) T. Shida, S. Iwata, *J. Phys. Chem.* **1971**, *75*, 2591; e) P. Balk, S. Debruijn, G. J. Hoijtink, *Recl. Trav. Chim. Pays-Bas* **1957**, *76*, 907–918.

Received: August 16, 2005
Revised: March 6, 2006

